

Partial cone crack formation in a brittle material loaded with a sliding spherical indenter

BY B. R. LAWN*

H. H. Wills Physics Laboratory, University of Bristol

(Communicated by F. C. Frank, F.R.S.—Received 24 October 1966)

[Plate 3]

In the preceding paper Frank & Lawn (1967) investigated theoretically the development of a cone crack in the strongly inhomogeneous Hertzian stress field. The analysis outlined in that paper is now extended to incorporate a sliding motion of the spherical indenter across the specimen surface, assuming a uniform coefficient of friction over the contact area. Sliding is found to have a large influence on the quasistatic stress field in the loaded specimen, and this in turn affects the ultimate geometry of the cracks. The precise shape of the partially developed cones thus formed is a function only of the Poisson ratio of the specimen material and the coefficient of friction. Criteria determining when surface fracture will occur, expressed as relationships between the critical normal load P_c acting on the specimen and the indenter radius r , are calculated as before. The Auerbach law found for purely normally loaded specimens, namely that P_c is proportional to r , over a certain range of r , should cease to hold when the coefficient of friction exceeds about 0.02. P_c then becomes very nearly proportional to r^2 , which corresponds to a critical stress criterion. The effect of sliding on the value of P_c becomes large with larger values of the coefficient of friction; this is of particular relevance to studies of the surface damage of brittle materials.

1. INTRODUCTION

The mechanism of cone crack formation in a brittle material loaded normally with a hard spherical indenter is more clearly understood when the inhomogeneous stress field through which the crack propagates is considered in detail (Frank & Lawn 1967, preceding paper). The criteria determining when a cone crack will develop, generally expressed as relations between critical normal load P_c and indenter radius r , follow directly from such considerations. It is of interest to attempt to extend the analysis to the case where the indenter is moved across the specimen surface at constant velocity. Under such conditions a composite track of approximately evenly spaced 'partial' cone cracks is formed when the critical normal load is attained. (The term 'partial' has found frequent usage in the literature because of the incompleting arcuate trace of each individual crack on the specimen surface.) These tracks have a fundamental relevance to mechanical properties, such as abrasion, of hard materials. This relevance indeed forms the basis for the experimental investigations of Preston (1922) on glass and Seal (1958) on diamond surfaces. Since the quasistatic stress field around a sliding contact area is well defined and has been solved analytically (Hamilton & Goodman 1966) we may proceed as before and determine the fracture conditions as the coefficient of friction f between indenter and flat surface varies. It will be seen that the frictional tractions exert an appreciable influence both upon these conditions and on the geometry of the partial cone cracks.

* Now at Division of Engineering, Brown University, Providence, Rhode Island, U.S.A.

The treatment below makes a few assumptions. The contact between indenter and specimen is taken to be free of 'stick-slip' motion (Mindlin 1949) and the indenter and specimen are taken to behave like purely elastic and elastic-brittle solids respectively. In many cases deviations from such idealized behaviour will occur; for instance, Bowden & Brookes (1966) have shown that the sliding action of an indenter may produce dislocation-nucleated cracks in magnesium oxide, a material generally regarded as highly brittle. However, such complications will be neglected in the following treatment.

2. STRESS FIELD AND CRACK GEOMETRY

In discussing the behaviour of crack propagation in an isotropic material we are concerned with the distribution of the maximum principal stress throughout the specimen: in a crystalline material the anisotropy of γ (surface energy of specimen) complicates the issue and crack propagation depends on the orientation of favourable cleavage planes in the stress field and on the stresses resolved along these planes. With regard to isotropic materials it was argued by Frank & Lawn (1967) that a crack in a strongly inhomogeneous stress field would tend to follow the surface defined by the two lesser of the three principal stresses, with the reservation that it would 'swing wide' on the bends where the trajectory surface became grossly curved. The evidence from studies on conventionally produced cone cracks showed excellent agreement with this hypothesis. A second feature necessary for a quantitative study of the fracture mechanism is that the ring crack initiate at or close to the circle of contact, where the tensile stress in the specimen reached its greatest value. This also has some experimental support. Both these features are readily extended to the case where an extra sliding motion of the indenter occurs. The position of greatest tensile stress still occurs on the circle of contact, for all f , at the trailing edge of the indenter. The distribution of the maximum principal stress, σ_1 , is shown in figure 1 for two values of f , 0.1 and 0.5 (Poisson's ratio ν taken to be $\frac{1}{3}$). It is noted that the tensile stress contours tend to crowd around the trailing edge as f increases, but correspondingly become less shallow beneath the surface. It was this shallow stress distribution which accounted for Auerbach's law for the normally loaded case. The value of the greatest tensile stress, from the analysis of Hamilton & Goodman, is given by

$$\sigma_m = (1 + 15.5f) \left(\frac{1}{2} - \nu\right) p_0, \quad (2.1)$$

where p_0 is the mean pressure $P/\pi a^2$, a being the radius of contact area, given in turn by

$$a^3 = \frac{4}{3} k P r / E \quad (2.2)$$

from the Hertz analysis. E is Young's modulus and k is defined by

$$k = \frac{9}{16} [(1 - \nu^2) + (E/E')(1 - \nu'^2)], \quad (2.3)$$

where the primes refer to the indenter material. k becomes unity if indenter and specimen are of the same substance, reducing to about 0.5 for an ideally rigid indenter.

Included in figure 1 are the stress trajectories of σ_3 as drawn from the point of σ_m . We note that they become less curved as f increases so we may regard, with increasing confidence, the σ_2 - σ_3 trajectory surface as a delineator of the crack path. The principal stress σ_2 , which for the case of zero friction was a 'hoop stress' with symmetry about the axis through the centre of contact, departs from this circular symmetry, as shown by traces of its trajectories on the specimen surface. This predicts that crack traces become less curved at higher values of f , and that the crack may not completely encircle the area of contact as the crack propagates into the region of reduced tensile stress. Further, since the tensile stresses beneath the specimen surface are relatively small near the front end of the indenter the likelihood of the cone crack developing into this region, except under excessive loading conditions, appears increasingly remote.

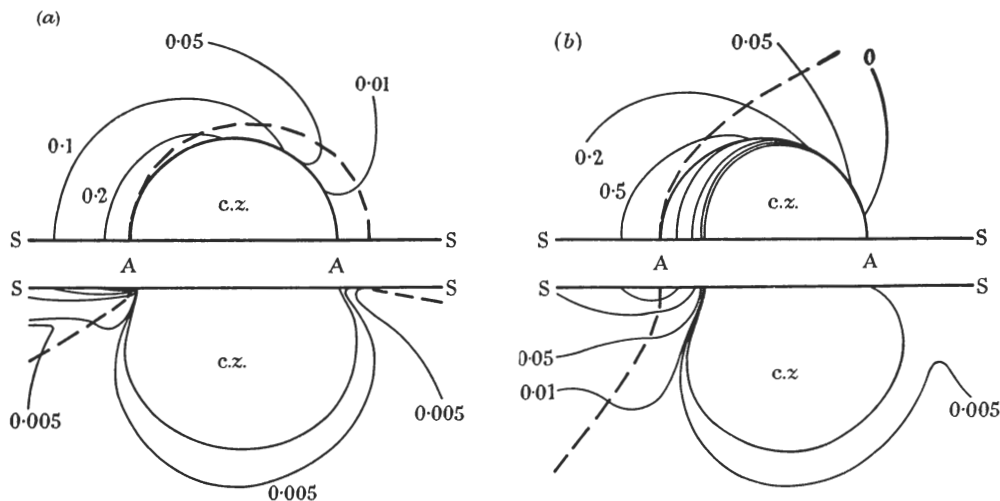


FIGURE 1. Half-surface view and side view of contours of greatest principal stress, σ_1 , in semi-infinite elastic medium (surface SS) in contact (diameter of contact AA) with spherical indenter. (a) $f = 0.1$, (b) $f = 0.5$. p_0 is the unit of stress. c.z. is the compressive zone in which all three principal stresses are negative. Broken lines are σ_2 (surface view) and σ_3 (side view) stress trajectories drawn from place of greatest tensile stress in the specimen. Indenter slides from left to right.

Experimental evidence is in excellent qualitative agreement with all above features of the hypothetical crack geometry, and we will therefore adopt these as a basis for establishing a more quantitative approach in § 3. A simple experiment will serve here to illustrate some of the details described above. Figure 2, plate 3, shows a partial ring crack produced by dropping a steel sphere, radius 0.875 cm, on to 1 in. thick plate glass inclined at about 45° to the horizontal, from a height of about 7 cm. The ball, being greased, has left a trace of the contact area, which, being very nearly circular, indicates that the ball has not slid far down the specimen surface. A detailed consideration of the mechanics of this arrangement suggests that the assumption that a superposed normal load and constant velocity sliding force operate at the instant of fracture is at least approximately satisfied. The fact that the contact between ball and glass was a well lubricated one suggests that the

coefficient of friction was low, probably about 0.1. Comparison of figure 2 with figure 5 in the paper by Frank & Lawn permits a ready appraisal of the effect of a small frictional force on the surface trace of a cone crack. Observation of the crack shown in figure 2 below the surface of the glass indeed showed the 'tail' of the crack to extend relatively deeply into the material from the trailing edge, at an angle to the surface roughly equal to that shown in figure 1(a) corresponding to $f = 0.1$. That the crack initiated from very near to the trailing edge of the indenter and grew downward and outward from this point may be inferred by a close examination of subsurface cracks. The precise location of the partial cone cracks with respect to their area of contact was generally subject to some statistical variation in much the same way as those discussed in the paper on conventionally produced cone cracks.

The familiar composite fracture tracks produced when indenters slide over a clean surface (§ 1) provide information on the effect of higher frictional tractions on crack geometry. Preston's classical descriptions of surface and cross-sectional traces of individual partial cone cracks comprising such fracture tracks on glass surfaces (Preston 1922) are in complete accord with the features of crack geometry indicated by the σ_2 and σ_3 stress trajectories in figure 1(b).

The principles of cone crack geometry discussed in this section may be applied, with caution, to the production of surface cracking in crystalline materials. A rigorous investigation of the mechanics of crack production must take into account the orientation of 'easy' cleavage planes with respect to the stress field, which in turn involves the direction of motion of the slider. Such an analysis is not considered here. However, we may note in passing the relative complexity of the crystalline case with reference to the example shown in figure 3. Here we see a 'chatter' track on an octahedron surface of a natural diamond. On the normally loaded octahedron surface of diamond it requires considerably less load to propagate a crack along a cleavage plane extending *away* from the compressive zone under the indenter. The ease of production of the scratch shown in figure 3, plate 3, therefore may depend a great deal on whether or not the cleavage plane whose surface trace lies perpendicular to the direction of motion of the scratching particle extends towards or away from this direction. A scratch in the opposite direction may be correspondingly easier or more difficult to produce.

3. FRACTURE CRITERIA

Having established a basis for calculating the prior stresses along the proposed crack path we may now proceed in a more quantitative manner. Before doing so we consider the following points concerning the crack path. First, the crack is taken to lie in a plane normal to the surface of the specimen. This assumption becomes unreliable when the length of the crack approaches the radius of curvature of the crack surface. Further, as f increases the gradient of tensile stress along the σ_2 trajectory becomes increasingly large, and will lead to further deviations from a situation of plane strain. However, as the fracture criteria are generally determined by the behaviour of the crack at lengths small compared with a , we may disregard these difficulties and merely treat the solutions at large crack lengths as rough indicators



FIGURE 3. Electron micrograph of replica taken from an octahedron surface of a natural diamond. Width of track about $1\ \mu\text{m}$. Direction of scratching from bottom left to top right of micrograph.

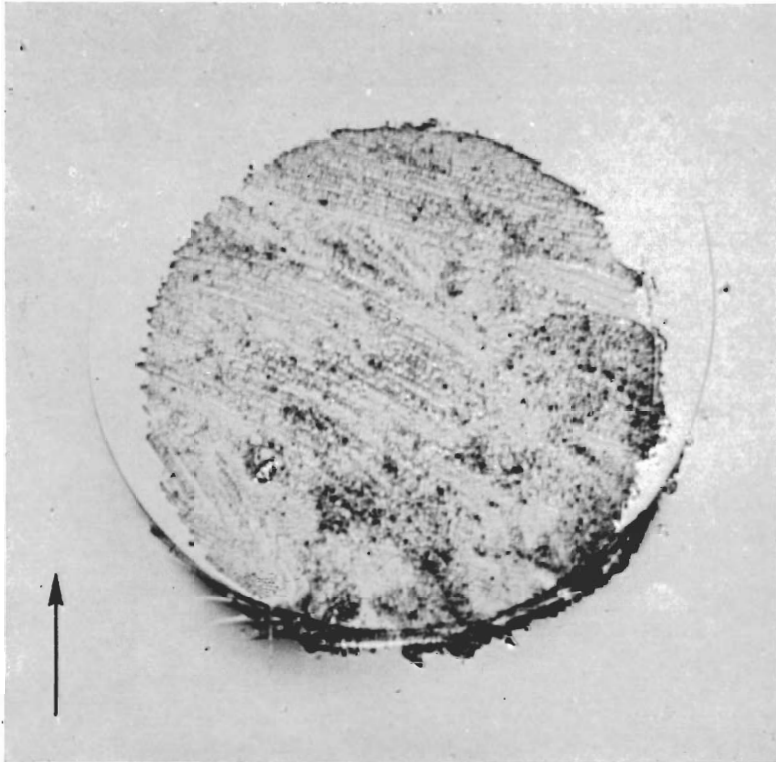


FIGURE 2. Surface view (reflected light) of partial cone crack formed by dropping a steel ball, radius $r = 0.875\ \text{cm}$, on to an inclined glass plate. Grease patch, radius $a = 0.049\ \text{cm}$, reveals area of contact. Arrow indicates line of impact.

of ultimate crack behaviour. We accordingly begin by considering the distribution of tensile stress σ_1 as a function of distance b along the σ_3 trajectory drawn from the trailing edge of the indenter: this is shown for four values of f in figure 4. The large influence of the frictional tractions is apparent, and it is pointed out that σ_1 falls off less steeply with b as f increases.

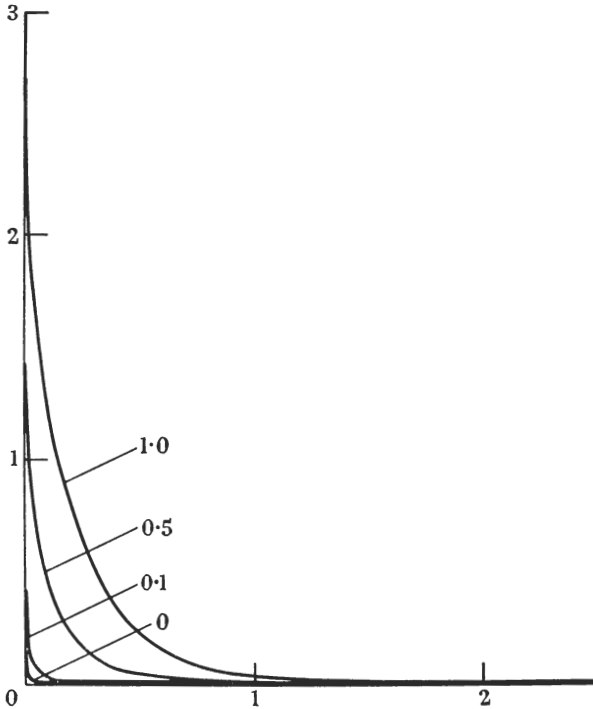


FIGURE 4. Plot of σ_1/p_0 as a function of relative distance b/a along crack path. Plots shown for $f = 0, 0.1, 0.5, 1.0$.

In Irwin's (1958) notation the Griffith (1920) condition that a crack will extend may be written

$$\mathcal{G} = (\pi/E)(1 - \nu^2) \mathcal{K}^2 > 2\gamma \tag{3.1}$$

for a surface crack of length c in a semi-infinite elastic medium, where \mathcal{G} is the strain energy release rate and \mathcal{K} is the stress intensity factor. For a plane crack loaded along its faces with normal prior stresses $\sigma(b)$ we have

$$\mathcal{K} = \frac{2}{\pi} c^{\frac{1}{2}} \int_0^c \frac{\sigma(b) db}{(c^2 - b^2)^{\frac{1}{2}}}.$$

We see from figures 1 and 4 that by expressing stresses in units of p_0 and lengths in units of a we need not consider the size of the indenter. Expressing the quantities in \mathcal{K} in terms of these units, and putting $\sigma_1 = \sigma(b)$, we obtain

$$\mathcal{K} = \frac{2}{\pi} \left(\frac{c}{a}\right)^{\frac{1}{2}} p_0 a^{\frac{1}{2}} \int_0^{c/a} \frac{\sigma_1/p_0 d(b/a)}{(c^2/a^2 - b^2/a^2)^{\frac{1}{2}}}. \tag{3.2}$$

As we shall see later we will be comparing the behaviour of crack propagation of the cone cracks with that of a Griffith-like crack. For this purpose it is convenient to write

$$I = \frac{2}{\pi} \frac{p_0}{\sigma_m} \int_0^{c/a} \frac{\sigma_1/p_0 d(b/a)}{(c^2/a^2 - b^2/a^2)^{1/2}}, \quad (3.3)$$

so that the integral I assumes the value unity for a Griffith crack ($\sigma_1 = \sigma_m = \text{constant}$). In general, because σ_1 is always less than σ_m except at $b = 0$, we will have

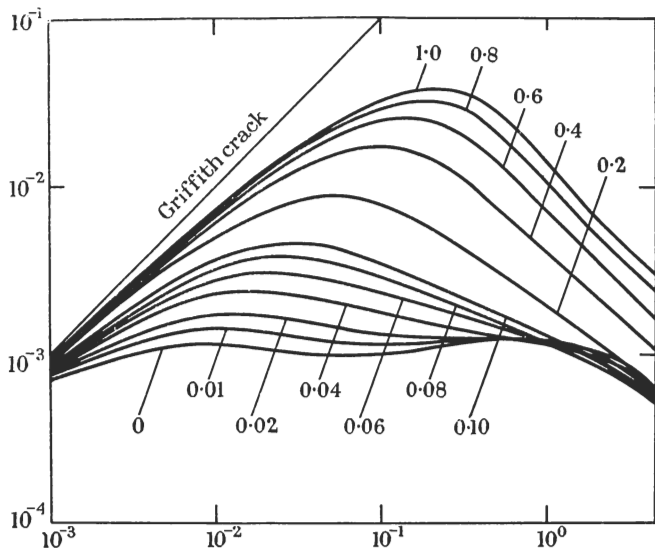


FIGURE 5. Plot of $(c/a)I^2$ as function of relative crack length c/a . Curves for various f values are shown, together with the straight line corresponding to a Griffith-like crack.

$I < 1$. The condition (3.1) may now be rewritten, with the aid of (3.3), (3.2) and (2.1), in the form

$$\frac{c}{a} I^2 > \frac{8}{\pi} \frac{\gamma E}{(1-\nu^2)(1-2\nu)^2} \frac{1}{(1+15.5f)^2} \frac{1}{p_0^2 a}.$$

Rearranging $p_0^2 a$, making use of (2.2), in the form

$$p_0^2 a = \frac{1}{\pi^2} \frac{3E}{4k} \frac{P}{r}, \quad (3.4)$$

we obtain

$$\frac{c}{a} I^2 > \frac{32\pi}{3} \frac{k\gamma}{(1-\nu^2)(1-2\nu)^2} \frac{1}{(1+15.5f)^2} \frac{r}{P}. \quad (3.5)$$

The quantity $(c/a)I^2$ may be regarded as a measure of the rate of release of strain energy as the crack extends. Plots of this quantity as a function of c/a , for various values of f , are shown in figure 5. On this graph the curve representing a Griffith-like crack is a straight line of slope unity: the curves for the partial cone cracks fall below this line, as expected. It is seen that the cracks, particularly those corresponding to higher f values, are more Griffith-like in behaviour at small c , all curves (necessarily) approaching each other to merge at the origin.

The phenomenon of crack growth may now be conveniently represented by the following graphical representation of (3.5). For a given indenter and specimen the right hand side of this inequality, being independent of (c/a) , may be drawn as a horizontal straight line in figure 5. Let us describe this horizontal line by its ordinate value H : we note that for a given load H is a function of material constants, the coefficient of friction, and the radius of the indenter, all of which are assumed to remain invariant for a given experiment. H , if it intersects the appropriate $(c/a)I^2$ curve at all, will do so in at least two places. In accordance with previous notation we will denote the values of crack length corresponding to these intersections as c_0 and c_3 , with $c_0 < c_3$. As seen from figure 5 there will, except for $f < 0.02$, be *only two* intersections. For the small exceptional range $0 < f < 0.02$ H may intersect the curve at two intermediate values of crack length, c_1 and c_2 . A crack of length c , with indenter load P , is then represented by a point $(c/a, H)$. The behaviour of the crack is determined by the location of this point in figure 5: three distinct types of crack behaviour may be distinguished. First, as P increases from zero $(c/a, H)$ migrates from (∞, ∞) down a straight line of slope three on the double-logarithmic plot (H being proportional to P^{-1} and c/a proportional to $P^{-\frac{1}{3}}$) toward the $(c/a)I^2$ curves. Until it intersects the appropriate curve the condition (3.5) remains unsatisfied and no crack extension can occur. The second and third types of crack behaviour therefore become realised when intersection occurs. If the slope of the $(c/a)I^2$ curve at this point is positive the crack will grow unstably along the H line, which represents crack extension under constant loading conditions. The crack will ultimately become arrested if $(c/a)I^2$ falls below H again (for the Griffith crack this will, of course, never occur). If, at intersection, the slope of the curve is negative, c will extend in a stable manner, following the $(c/a)I^2$ curve as the load is increased (and H is depressed), until such stage as the slope becomes positive and the crack becomes unstable again.

The treatment above requires the presence of a crack prior to loading: pre-existing microscopic flaws, c_f in length, must now be invoked, as in the Griffith treatment, to explain the observed behaviour. The load is then increased until the condition $(c_f/a)I^2 > H$ is satisfied. Treating first the range $f > 0.02$ we see that if $c_f = c_0$ when this condition is achieved the crack will become unstable and grow (under constant load) to the stable length c_3 , until the curve falls below the H line again. If, however, $c_f = c_3$, the crack is already stable, and will grow only if the load is increased still further. Writing P_c for the critical load required to satisfy the fracture criterion above, and eliminating a (using (2.2)), we have

$$\frac{P_c}{r^2} = \frac{256\sqrt{(2\pi^3)}}{9} \frac{k^2\gamma^{\frac{3}{2}}}{E^{\frac{1}{2}}(1-\nu^2)^{\frac{3}{2}}(1-2\nu)^3} \frac{1}{(1+15.5f)^3} \frac{1}{I_f} \frac{1}{c_f^{\frac{3}{2}}} \tag{3.6}$$

For the Griffith-like crack I_f is unity and the right hand side of (3.6) is independent of loading conditions. P_c/r^2 is then constant, and (3.6) corresponds to a critical stress criterion for fracture. However, we observe that I_f is, in reality, a function of H , and therefore of P_c , in such a way that P_c becomes proportional to r^{2-n} . If, as is generally realized in practice, $c_f \ll a$, the cracks will behave in a near Griffith-like manner, and n will not deviate excessively from zero. Turning now to the range $f < 0.02$ we find

that, for a certain range of c_t , we have four intersections of H with the curves in figure 5. If, in this range, $c_t = c_0$ when the fracture criterion (3.5) is satisfied, the crack will proceed unstably to c_1 . In the preceding paper it was pointed out that the stable crack c_1 passes unobserved: to produce a visible crack H must therefore be depressed below the minimum in the $(c/a)I^2$ curve. The length c^* of the crack corresponding to this minimum (the asterisk will hereafter be used to denote any quantity corresponding to $c = c^*$) is, unlike c_t , proportional to a : this explains the difference between the Griffith-like behaviour discussed above and the present (Auerbach) behaviour. Writing, for the latter, $[(c/a)I^2]^* (= \text{constant}) > H$, we have

$$\frac{P^*}{r} = \frac{32\pi}{3} \frac{k\gamma}{(1-\nu^2)(1-2\nu)^2} \frac{1}{(1+15.5f)^2} \frac{1}{[(c/a)I^2]^*}. \quad (3.7)$$

Since the Auerbach-like crack is of relatively little relevance here it will not be discussed to any great extent.

Since we are interested in the relative ease of surface crack production on materials due to a normally loaded and a sliding indenter it is convenient to express P_c in terms of the static load P_0^* (i.e. with $f = 0$) required to produce a conventional cone fracture within the limit of validity of Auerbach's law. Comparing (3.7) with (3.6), and evaluating the numerical factor $[(c/a)I^2]^*$ from figure 5, we have

$$\frac{P_c}{P_0^*} = 6.7 \times 10^{-3} \frac{k(\gamma/E)^{\frac{1}{2}}}{(1-\nu^2)^{\frac{1}{2}}(1-2\nu)} \frac{1}{(1+15.5f)^3} \frac{r}{I_f^3 c_f^{\frac{3}{2}}}. \quad (3.8)$$

Taking, for a steel ball sliding on glass, $\gamma = 500 \text{ erg/cm}^2$, $E = 7 \times 10^{11} \text{ dyn/cm}^2$, $c_f \sim 1 \times 10^{-4} \text{ cm}$, $k \sim \frac{2}{3}$, $\nu = \frac{1}{3}$, $I_f^3 \sim \frac{1}{2}$, $r = 0.3 \text{ cm}$, (3.8) reduces to

$$P_c \sim 0.2P_0^*/(1+15.5f)^3,$$

so long as $f > 0.02$. This predicts that for a coefficient of friction as low as 0.1 the load necessary to initiate cone fracture may well be reduced by a factor of 100 or more. For smaller radius indenters this factor will increase still further: this last fact has implications when abrasion mechanisms are considered.

4. DISCUSSION

In § 2 it was shown that the σ_2 - σ_3 stress trajectory surface, drawn through the position of greatest tensile stress in the specimen, gives a reasonably faithful indication of the ultimate shape of a partial cone crack. In this treatment σ_1 was assumed to be always the greatest principal stress: within the region around the indenter illustrated in figure 1 this assumption is never violated. However, for crack lengths $c \gg a$, σ_2 may become at least comparable with σ_1 , especially for large f , and may lead to complications in crack geometry if the crack becomes deflected from its initial, well defined path. Some of Preston's photographs of surface traces of partial cone cracks show a related secondary effect; they reveal a second set of cracks whose individual members intersect the primary cracks discussed in § 2 very nearly orthogonally, as if their direction were dictated by the σ_1 trajectories (that is, by the σ_2 stresses). Although σ_2 is relatively small compared with σ_1 it is positive in the region where the secondary cracks appear, for $f \sim 0.5$; a full understanding of these cracks is not within the scope of the present treatment.

Equation (3.8) demonstrated that the introduction of a sliding motion to a normally loaded spherical indenter, on a brittle surface, significantly increases the ease of production of a partial cone fracture. This occurs for two reasons; first, because sliding increases the tensile stresses in the wake of the indenter; and, secondly, because, for f greater than about 0.02, the crack no longer requires to satisfy the Auerbach criterion, the latter requiring additional load to push the stable crack c_1 past c^* . Quantitative verification of this treatment is difficult to obtain because of experimental deviations from the idealized situation assumed in §1. Most published work has been performed on glass surfaces; if the indenter is harder than the glass some plastic grooving on the specimen surface, due to prominent asperities on the slider, is often observed, while if the indenter is relatively soft some adhesion, via plastic junctions, may occur. These effects will tend to violate the validity of the Hertzian elastic analysis. The second effect was observed by Ghering & Turnbull (1940), who measured the minimum load required to scratch glass surfaces with hemispherically tipped metal rods. Metal traces were left on the scratched glass surfaces, and the indenters were observed to have deformed noticeably after the experiments, which almost certainly means that the quoted critical loads are over-estimates. For instance, for a steel rod of tip radius 0.3 cm the critical load required to produce a fracture track was 0.23 Kg. From the data of Preston (1945) (Preston's experiments were performed in the same laboratories, and, presumably, on similar glasses to those of Ghering & Turnbull) the critical load P_0^* required to induce a cone crack under purely normal loading, for a steel ball of the same radius as used by Ghering & Turnbull, is about 35 Kg. Thus the effect of sliding is to reduce the critical load required to produce visible cone fracture by a factor of about 150. Equation (3.8) (and the use of the values cited for the parameters in the example illustrating this equation) would give agreement with this factor if f were to be about 0.14. Southwick (1958), quoted by Holland (1964), measured f for steel on glass, under similar experimental conditions, and found a value of 0.6, but he used a larger radius hemispherical tip and a larger applied load than Ghering & Turnbull, both of which would tend to increase f . However, the real coefficient is not likely to be as low as 0.14, and the reason for the discrepancy between experiment and theory may be due to either the deformed indenter, as mentioned above, or the gross uncertainty of the parameters inserted into (3.8), or a combination of both, or to the inadequacy of the assumptions in developing the theory. In any case the point emphasized by the theoretical treatment, that sliding is of utmost importance when considering surface damage, does have at least some qualitative experimental backing.

Finally, it is pointed out that brittle materials may easily suffer surface damage when small particles rub across their surface under reasonably small loads. Thus the scratch on the diamond surface shown in figure 3 may well have originated as the stone went through its mining process, and may have been caused by a particle considerably softer than diamond itself (Tolansky & Howes 1957). Such surface cracks will not heal perfectly and the surrounding crystal will be left in a state of residual elastic stress (Lawn & Komatsu 1966). The cumulative effects of many scratches may therefore introduce considerable surface compression. This effect is

vividly demonstrated by X-ray topographs of diamonds whose surfaces have been subjected to micro-abrasion tests (Frank, Lang, Lawn & Wilks, in preparation).

The author wishes to express his gratitude to Professor F. C. Frank, F.R.S., for his interest in this work and for numerous discussions. He is also indebted to Industrial Distributors Ltd. for a Research Fellowship.

REFERENCES

- Bowden, F. P. & Brookes, C. A. 1966 *Proc. Roy. Soc. A* **295**, 244.
Frank, F. C. & Lawn, B. R. 1967 *Proc. Roy. Soc. A* **299**, 291.
Ghering, L. G. & Turnbull, J. C. 1940 *Bull. Am. Ceram. Soc.* **19**, 290.
Griffith, A. A. 1920 *Phil. Trans. A* **221**, 163.
Hamilton, G. M. & Goodman, L. E. 1966 *J. Appl. Mech.* **33**, 371.
Holland, L. 1964 *The properties of glass surfaces*. London: Chapman and Hall.
Irwin, G. R. 1958 *Handbuch Physik* **6**, 551. Berlin: Springer.
Lawn, B. R. & Komatsu, H. 1966 *Phil. Mag.* **14**, 689.
Mindlin, R. D. 1949 *J. Appl. Mech.* **16**, 259.
Preston, F. W. 1945 *J. Am. Ceram. Soc.* **28**, 145.
Preston, F. W. 1922 *Trans. Opt. Soc.* **23**, 141.
Seal, M. 1958 *Proc. Roy. Soc. A* **248**, 379.
Southwick, R. D. 1958 Friction and surface damage in a sliding metal to glass contact. *Preston Lab. Rep. no. 58-035*. Butler, Pennsylvania.
Tolansky, S. & Howes, V. R. 1957 *Proc. Phys. Soc. B* **70**, 521.